

NATIONAAL LUCHT- EN RUIMTEVAARTLABORATORIUM

NATIONAL AEROSPACE LABORATORY NLR

THE NETHERLANDS

NLR MP 83036 U

HALF-MODEL TESTING IN THE NLR HIGH SPEED TUNNEL HST: ITS TECHNIQUE AND APPLICATION

BY

S.J. BOERSEN AND A. ELSENAAR

Bibliotheek TU Delft
Faculteit der Luchtvaart- en Ruimtevaarttechniek
Kluyverweg 1
2629 HS Delft



NLR MP 83036 U

HALF-MODEL TESTING IN THE NLR HIGH SPEED TUNNEL HST
ITS TECHNIQUE AND APPLICATION

by

S.J. Boersen and A. Elsenaar

Paper presented at the AGARD Fluid Dynamic Panel Symposium on Wind Tunnels and Testing Techniques, 26-29 September 1983, Çeşme, Turkey.

Division: Fluid Dynamics

Prepared: SJB/*h* AE/*AE*

Approved: JHvdZ/*AE*

Completed : 830715

Ordernumber: 22.403

Typ. : PTP/

-2-
CONTENTS

	Page
1 INTRODUCTION	3
2 HALF/COMPLETE-MODEL COMPARISON	3
2.1 Possibilities for a systematic comparison	3
2.2 Half-model mounting	3
2.3 Wall interference	4
2.4 Wing characteristics	5
3 SOME TYPICAL APPLICATIONS OF HALF-MODEL TESTING	5
3.1 Reynolds number studies	5
3.2 Drag evaluation	6
3.3 Buffet tests	6
3.4 Wing/engine interference studies	6
4 CONCLUSIONS	7
5 REFERENCES	7
1 Table	8
27 Figures	9

(17 pages in total)

HALF-MODEL TESTING IN THE NLR HIGH SPEED WIND TUNNEL HST:
ITS TECHNIQUE AND APPLICATION

by

S.J. Boersen and A. Elsenaar

National Aerospace Laboratory NLR
Anthony Fokkerweg 2
1059 CM Amsterdam
The Netherlands

SUMMARY

An evaluation is presented of the half-model test technique based on a systematic comparison of half-model test results with the corresponding full-model data. It is shown that the most important problems with this technique originate from half-model mounting and wall interference effects. At present, these effects can only be determined empirically using the full-model test results as a reference. It can then be shown that the pressure distribution on the wing and the off-design boundaries are well represented in the half-model tests. Finally, some typical applications of this technique, in which half-model test results are used on a relative basis, are presented.

1. INTRODUCTION

In the spectrum of wind tunnel test techniques half-model testing has acquired a prominent position. The advantages are clear: large models are attractive from the point of view of model construction, representation of geometrical detail and increased Reynolds number capability. Well known disadvantages are mounting effects and increased wall interference while the flight regime is restricted to symmetrical conditions only.

As a result of the continued interest from industry in half-model testing an investigation was started at NLR some 5 years ago to determine the main problem areas and to improve upon the existing technique as put in practice in the NLR High Speed Wind Tunnel HST at that time. The HST is a variable pressure transonic wind tunnel with test section dimensions of 1.6 x 2 meters (ref. 1). Full-span models of transport type configurations usually have a span of about 1.2 meter, yielding a Reynolds number performance as indicated in figure 1. The same figure also shows the increased Reynolds number capability when the larger size of half-models is fully exploited. Still higher values of the chord Reynolds number can be achieved with the two-dimensional set-up, as recently put into use in the HST (ref. 2,3). It is the interest in high Reynolds number research that has prompted the present investigation of the half-model test technique.

2. HALF/COMPLETE-MODEL COMPARISON

2.1 Possibilities for a systematic comparison

It was felt that an evaluation of the half-model test technique was only feasible from a systematic comparison of half-model test results with those obtained on a full-span model of identical shape. The HST is very suitable for such a comparison since the variable stagnation pressure can be adjusted such as to obtain the same Reynolds number on the much smaller full-model. 5 different models have been compared (table 1), mainly for "clean" wing configurations. Low speed configurations with flaps and slats have been included however. A typical example of a half-model and the corresponding full-model as mounted in the HST is shown in figure 2.

In the evaluation overall force and moment coefficients were compared whereas local pressure distributions were used to investigate the observed differences in more detail. It is assumed that the results of the full-models are free of wall interference effects. Numerous comparisons (e.g. refs. 4,5 and 6) of one model in various wind tunnels have shown this assumption to be valid. The comparison of forces is hampered to some extent by loss of accuracy in the half-model data at low stagnation pressures, the balance being selected for high Reynolds number tests. In general, the half-models were sufficiently identical to the corresponding full model to warrant a proper comparison. Wing deformation must be taken into account however. This can be estimated from calculations for clean wing configurations. For more complex configurations with high lift devices such an estimate is almost impossible.

It is the aim of the comparisons as presented hereafter, to reveal the origins of the observed differences and to indicate ways of improvement. It is still more important to prove that half-model test results are meaningful (see e.g. ref. 7) and this will be discussed at the end of this chapter.

2.2 Half-model mounting

Ideally half-model mounting should be such that the wall on which the model is mounted acts as a perfect reflexion plane. From experience, it was considered essential to avoid mechanical contact other than the model-balance connection. To prevent interference due to secondary flow between the half-body and the tunnel side wall, a labyrinth seal was applied around the entire circumference of the body (fig.3). However, this solution does not eliminate all unwanted aerodynamic interference. To reduce tunnel wall boundary layer effects on the flow over the half-model fuselage very often a splitter plate or some form of boundary layer control (see e.g. ref. 8) is used. At NLR this approach has not been followed.

Between the half-body and the tunnel wall only a so-called boundary layer plate is mounted to compensate for the boundary layer displacement thickness and to accommodate the labyrinth seal (fig. 3).

Half-model mounting effects can be assessed from a comparison with the corresponding full-models for "body-alone" configurations. The results of such a comparison are shown for 4 different models in figure 4 as differences in tangential force C_T . The upper part of this figure reveals very large variations in axial force differences as a function of incidence. The Mach number dependence is also quite substantial, but similar for all models tested. This effect can partly be explained from changes in the local pressure field near the nose caused by the boundary layer plate and the flow of the tunnel wall boundary layer over and around the model. It must be remarked here that the boundary layer plate for the models 3 and 4 was about three times as thick as the one applied on the other models and this will certainly effect the location of the stagnation point in the nose region, introducing large pressure drag effects. However, tunnel wall induced axial pressure gradients are also of importance. This is illustrated with figure 5 where the pressure distribution over the front and rear part of the half-model is compared with the corresponding results for the full-model. The observed axial pressure gradient is a tunnel wall interference effect, directly related to the half-model size relative to the length of the slotted part of the test section. The large geometrical blockage of the half-model (from 2 to 4%) introduces pressure gradients near the transition from the solid to the slotted test section walls. The figure also illustrates that the pressure differences are almost absent near the wing location indicating that the wing itself will experience the approximately correct Mach number. These "buoyancy-type" effects cannot, at present, be determined from a theoretical wall interference correction method. So far the C_T -comparison of the "body-alone" configuration has been discussed. One might wonder if the observed effects of fuselage mounting and wall-induced axial pressure gradients change when a lifting wing is added to the fuselage. This can be assessed from a C_N-C_T comparison of the complete (wing + fuselage) configurations after the measured "body-alone" differences in C_N and C_T (at the same angle of incidence) between the full- and half-model are subtracted. A typical example of such a comparison is shown in figure 6. The resulting C_T -differences are now in the order of 20 counts and only weakly lift and Mach number dependent. The observed shift is most likely due to the increased solid blockage when the wing is added causing an increased axial pressure gradient over the half-model nose as already observed on the fuselage (fig. 5). Ideally the C_N-C_T curves should collapse (when geometrical differences, including wing deformation can be neglected) and the observed differences are indicative of the accuracy that can be obtained in tangential force with half-model tests. There clearly is a need for improvement.

2.3 Wall interference

In view of the large model dimensions for half-model tests, one should anticipate appreciable wall interference effects. The wall interference effect can be expressed as a correction in Mach number (or dynamic pressure) and in angle of incidence at the model reference location. Additionally, flow non-uniformities that can be expressed as spatial variations in static pressure and upwash may be introduced by the tunnel walls. In section 2.2 it was already shown that static pressure gradients greatly effect the axial force on the half-model body.

For the half-model tests, wall interference effects have been assessed empirically from a comparison with full-model tests. Wall interference on dynamic pressure q (or Mach number) at the wing location can be estimated from a comparison of the average of the upper and lower surface pressures (\bar{C}_p) for a number of spanwise pressure stations. It can then be shown that:

$$\frac{\Delta q}{q} = \frac{2 - Ma^2}{2 - \bar{C}_p (2 - Ma^2)} \cdot \Delta \bar{C}_p$$

where Δ represents the difference between half- and full-model results. Typical examples are shown in the figures 7 and 8. All models show a negligible difference at zero lift (in accordance with the results of the "body-alone tests", fig. 5) and an almost linear increase with lift. An average line, derived from comparisons on three different models, is presented in figure 9 in terms of the wall interference parameter $C_{L,ref}/S_{tunnel}$. In the same figure the calculated wall interference effect for a two-dimensional model as tested in the HST is depicted. In this case the wall interference could be calculated with the measured boundary condition method of ref. 9. The two sets of results are very much alike and they indicate an appreciable effect of the lift on the wall interference for these large models. Near the design condition of a transport type aircraft the effect on Mach number is of the order of 0.005; at low-speed, high-lift conditions the C_L -max value may change as much as 5%.

The wall interference effect on angle of incidence can be deduced from a comparison of lift curve slopes after corrections for model deformation and wall interference on dynamic pressure are applied. Such a comparison, expressed as $a_1 = \Delta\alpha/C_N$ is shown in figure 10 for all models tested. The interference effect is quite large and similar for models with about the same wing area. For model 2, with a much smaller wing area, the effect is smaller as well.

The observed differences in lift curve slope appear to be almost entirely due to a change in the angle of incidence as can be assessed from a comparison of local lift-curve slopes obtained from sectional pressure integration (fig. 11); Note that in this comparison the angle of incidence of the half-model is corrected according to fig. 10). The curves are almost identical near the wing root. Further out to the wing tip, differences in lift-curve slope become more pronounced. They can be explained from differences in wing deformation (the full-model experiences more deformation than the half-model due to the higher dynamic pressure required for the full-model to obtain equal Reynolds numbers). These results also indicate that a spatial variation along the wing span of tunnel wall induced upwash is almost absent.

One other problem should be noted with respect to the angle of incidence. Since tests on an inverted half-model are not practical, the zero-lift upwash angle can only be estimated from a comparison with the full-model results. Such a comparison for the tested models is also shown in figure 10. It shows an appreciable scatter around zero degree also indicating that the accuracy of half-model testing in this respect is clearly inferior as compared to full-model results. Note also that model deformation and model differences will show up very pronouncedly in this figure.

This section should be concluded with the remark that wall-interference effects do represent an important problem in half-model testing. For further improvements of the half-model technique, reliable theoretical wall interference correction methods must be available. Measured boundary condition methods are the most promising in this respect.

2.4 Wing characteristics

The two previous sections have shown important effects of half-model mounting and wall interference. These effects result in large uncertainties in tangential force and free stream conditions that deteriorate the absolute value of half-model tests. However, assuming that appropriate corrections can be made for these effects, it still remains to be answered how closely the flow over the half-model wing resembles the flow over the corresponding full-model. Therefore, in this section comparisons of some aerodynamic characteristics will be shown to validate the value of half-model tests.

For this final comparison, the following pragmatic procedure* has been adopted:

- 1) the half-model test results have been corrected for the measured force differences between the body-alone configurations in terms of ΔC_T , ΔC_N and ΔC_m at the corresponding angle of incidence;
- 2) the empirical dynamic pressure correction as described in section 2.3 has been applied (see also fig. 9);
- 3) the empirical angle of incidence correction, derived from a comparison of a half-model and a full-model configuration has been applied after appropriate corrections for model deformation (see fig. 10).

This procedure pre-supposes additional "body-alone" tests on the half- and full-model and additional reference measurements on the full-model for one typical configuration. For this configuration always a clean wing with fixed boundary layer transition was taken. It is assumed that the so derived "corrections" can be applied to other configurations as well.

Figure 12 and 13 show a comparison of pressure distributions for a subsonic and transonic ("design") condition. It shows that the pressure distribution is fairly well represented in the half-model tests, apart from a change in spanwise load-distribution caused by the larger wing deformation of the full-model (fig. 14). A similar agreement was found for the other models. A comparison of local C_{ℓ} - α curves was already shown in figure 11. Since the linear part of the (balance measured) C_L - α curves is effectively matched in the "correction" procedure, good agreement in lift-curves is evident. However, also the C_L - C_m curves generally compare very well. With the above described "correction" procedure typical C_m -differences as presented in figure 6 are also indicative for the remaining differences in drag. One other example of a drag comparison is shown in figure 15 related to a low-speed, high-lift condition. In this case the α -correction was derived solely from a clean wing comparison as given in figure 10. This half-model result of the HST has been compared with the corresponding result of a full-model (one half of it identical to the half-model) tested in the NLR low speed tunnel.

Finally, some off-design boundaries are compared. Figure 16 shows a typical comparison of maximum lift and buffet onset boundaries for a clean wing configuration. For this configuration the wall-induced q -effects will be small. In the high-speed regime also lift- and drag-divergence boundaries are compared (figure 17). As was the case for the clean wing C_L -max there is a fair agreement and it can be concluded that the shock-wave and separation development is well represented on the half-model wing. Similar results on the other models give enough confidence for the application of half-model testing on a relative basis. Some typical examples of such applications will be discussed in the next section.

3. SOME TYPICAL APPLICATIONS OF HALF-MODEL TESTING

3.1 Reynolds number studies

The large model-scales that can be realized with half-models make them particularly attractive for Reynolds number studies. A number of such studies have been made during recent years in the HST, where it is possible to study low-speed and high-speed configurations with one and the same model. In the low speed regime Reynolds number effects on drag and maximum lift are of particular interest. As discussed before, one must be cautious with balance-measured drag results obtained from half-model testing. The figures 6 and 15 gave already some indication of the absolute accuracy that can be obtained. Drag results, however, will be more reliable when used on a relative basis. Figure 18 shows such a comparison of drag increments due to slat and flap deflection measured on a full- and half-model at the same Reynolds number. It is well known that Reynolds number effects on low speed maximum lift can vary widely from one configuration to the other, while also the trend with Reynolds number may be highly non-linear. As discussed in section 2.3 the absolute value of C_L -max will be influenced to some extent by lift-dependent blockage effects. Reynolds number effects on maximum lift, however, may still be determined from half-model tests if it is assumed that wall-interference effects are independent of Reynolds number.

* Because more information became available in time, the full procedure has not been applied for all models tested.

Figure 19 shows a comparison of Reynolds number trends for the overall (balance measured) and local (pressure integrated) maximum lift values as measured on a full- and corresponding half-model for a clean wing configuration. A similar comparison in overall maximum lift is presented in figure 20 for configurations with high-lift devices. The agreement in an absolute sense is less satisfactory in this case, but Reynolds number trends compare very well. In the high speed regime, where C_{Lmax} values are much lower, a good correspondence in off-design boundaries is found (fig. 16 and 17) and trends with Reynolds number are expected to be well represented as well. The question whether wall interference effects are Reynolds number independent, is a very important one, and not typical for half-model testing. The question cannot be answered until reliable 3-D wall interference correction methods are available. An indication that the problem is a real one is given in figure 21 where for a 2-D model in the HST (50 cm chord) wall interference corrections have been presented as calculated with the measured boundary condition method of ref. 9 for two Reynolds numbers. Although the effects are relatively small ($\Delta M < .002$, $\Delta \alpha < .05^\circ$) they are still substantial when compared with some of the observed Reynolds number effects. There certainly is a problem!

3.2 Drag evaluation

In view of some loss of accuracy in balance measured drag on half-models, the half-model test technique cannot be recommended for accurate overall drag evaluation. However, the increased model size makes it attractive to use wake surveys for a much more detailed drag evaluation. This technique is to some extent open to criticism for 3-D configurations since, due to 3-D effects, the correspondence between the flow over a particular wing section and the downstream wake is lost. However, the measured total-head loss in the wake is still a measure of the drag force and 3-D effects will be small for high aspect ratio wings with attached flow. This technique has been applied successfully on a number of half-model tests and some typical results will be shown next. In figure 22 a drag brake-down is given for a transport type aircraft near the design Mach-number. The following drag-contributions can be distinguished:

- . fuselage drag from body-alone tests (full-model fuselage measured on a balance)
- . wing profile drag as measured from a wake rake survey behind the half-model wing using spanwise integration
- . induced drag calculated from the measured spanwise loading

The sum of these contributions is compared with the drag measured on the full-model. The differences in this case are very small, especially when noted that wing-body interference is not accounted for. The example illustrates the value of the wake survey technique. For the aircraft designer detailed information with respect to the drag brake down along the wing span is of more relevance. Figure 23 shows a typical example. In this case a low and high estimate of the wave drag (deduced from the total-head loss distribution outside the viscous wake) was made. It shows, at the higher lift coefficient an important reduction in wave drag with Reynolds number for the outer wing. The example shows that wake surveys may be useful for an evaluation of Reynolds number effects on drag in providing more detailed information on the drag brake-down that could not be obtained with sufficient detail from full-model tests.

3.3 Buffet tests

Half-model tests have successfully been used for the measurement of buffet intensity on fighter configurations. In these tests the method of Jones (ref. 10) has been used. This method is based on the notion that the lower and more important modes of vibration of a conventional wind tunnel model are similar to those of the aircraft. In the wind tunnel the aerodynamic excitation, the total damping and the structural damping of the model are measured. When the structural damping of the real aircraft is known, the buffet intensity in flight can be predicted. An important advantage of this type of measurements is that a rather conventional wind tunnel model can be used. The method is very suitable for half-models since the model support can be made very stiff. This reduces the possible occurrence of additional modes of vibration due to the model mounting with frequencies close to the dominant first bending mode, whereas also the structural damping can be kept sufficiently low. In the tests reported in reference 11 the structural damping was less than 15% of the total damping. Buffet-measurements on large half-models are particularly attractive since buffet boundaries are strongly Reynolds number dependent. In the above cited reference 11, related to a fighter configuration, the flight Reynolds number could almost be duplicated in the wind tunnel. Typical results are presented in figure 24 taken from this reference. The disagreement at the highest Mach number cannot be explained at present, but it is unlikely that the half-model test technique is to blame.

3.4 Wing/engine interference studies

The interference of wing-mounted engines with the flow over the wing is of great practical significance. Experimental studies are rather difficult due to model construction limitations and half-model tests have a definite advantage in this respect. Two examples of such tests in the HST are discussed in more detail in ref. 12 and 13. In the former case hydrogen peroxyde was used to simulate the core flow, whereas the fan flow was simulated by blown air. Detailed pressure measurements have been made in this case on the wing and near the engine (fig. 25) for a fixed engine location and a range of flow conditions. In the latter case a blown nacelle, with a faired inlet, was mounted on a separate strut (fig. 26). This arrangement was particularly selected to study the effects of a variation in engine position relative to the wing. In total 6 different locations have been studied in this way. The numerous pressure plotting stations provided detailed information of the flow field. It is worth noting here that in both examples relative drag and lift forces have been obtained from pressure integration mainly. An indication of the value of this procedure for the latter case can be found in figure 27 taken from ref. 13, where a direct comparison has been made of the relative lift and drag forces on a part of the model (wing and pylon only) from pressure integration and balance measurements. A direct measurement of thrust-minus-drag on the balance has, as yet, not been made in the HST. However, in view of the increased understanding of half-model drag results, direct force measurements, with a blown nacelle or TPS, appear to be feasible when made on a relative basis (study of outlet configuration changes, effects of pressure ratio variation, etc.).

4. CONCLUSIONS

In this paper some 5 years of experience with half-model testing in the HST is reported. From a systematic evaluation of a number of different models it could be established that the largest uncertainty in the application of this technique (for HST conditions) is caused by important wall interference effects, caused by the large model dimensions. In absence of a reliable 3-D wall interference correction method, the magnitude of these effects has been deduced from a comparison with corresponding full-model tests at the same Reynolds number. Wall-induced static pressure gradients along the fuselage length are the cause of substantial buoyancy forces. This introduces, in combination with model mounting effects, important deviations in the axial force as experienced by the half-model fuselage. The magnitude of these effects could be established from a comparison with corresponding full-model "body-alone" tests. Using this rather pragmatic approach, in which the half-model test results have been empirically corrected for wall interference and wall mounting effects, it could be established that the flow over the wing itself gives a good representation of the corresponding flow over the full-model wing. Pressure distributions and off-design boundaries are accurately represented. Drag values, however, are less accurate and can only be used on a relative basis. This limits, at present, the application of the half-model technique to a special class of dedicated experiments, where the main advantages of the half-model technique (increased model size, increased Reynolds number capability, rigid model mounting) can be fully exploited. This is illustrated with some typical examples e.g. Reynolds number studies, wake-drag evaluation, buffet tests and wing/engine interference studies. For each of these cases experimental limitations and benefits are shown.

5. REFERENCES

1. - User's Guide to the 1.6 x 2 m²
High Speed Wind Tunnel HST
2. Rozendal, D. Two-dimensional testing in the HST
Memorandum AC-83-021 U (1983)
3. Vogelaar, H.L.J. Description and validation of the
two-dimensional test set-up for
multiple airfoils in the
pressurized wind tunnel HST
NLR TR-83-031 U (1983)
4. Poisson-Quinton, Ph.
Vaucheret, X. Prediction of aerodynamic characteristics
from a correlation of results on
a calibration model tested in
various large wind tunnels
AGARD CP-242 (1977)
5. Boersen, S.J. Comparison of low-speed test results from
NLR-HST and ONERA-F1 wind tunnels
NLR report, to be published
6. - Comparative tests on the F-4 model
GARTEur Action Group AD(AG-01)
to be published
7. Bippes, H.
Turk, M. Half Model Testing Applied to
Wings above and below Stall from
"Recent Contributions to Fluid Mechanics",
Springer Verlag, 1982
8. Koppenwallner, G.
Szodruch, J. Bericht über die Sitzung des
DGLR-Fachausschusses 3.4
"Versuchswesen der Fluid- und
Thermodynamik"
DFVLR, IB 222-82 A. 35, Dezember 1982
9. Smith, J. A method for determining 2-D wall interference
on an airfoil from measured pressure
distributions near the walls and on the model
NLR TR-81-016 U (1981)
10. Butler, J.F.
Spavins, G.R. Preliminary investigation of a technique for
predicting buffet loads in flight from
wind-tunnel measurements on model of
conventional construction
AGARD CP-204, paper 24, September 1976
11. Teige, S.H., Nilsson, B.S.A.
Boersen, S.J., Kraan, A.N. Comparison of flight and wind tunnel
buffeting measurements on the
SAAB 105 Aircraft
AGARD CP-339, paper 12, October 1982
12. Munniksma, B.
Jaarsma, F. Jet interference of a podded engine
installation at cruise conditions
AGARD CP-150, March 1975

13. v. Engelen, J.A.J.
Munniksma, B.
Elsenaar, A.

Evaluation of an experimental technique to
investigate the effects of the engine position
on engine/pylon/wing interference
AGARD CP-301, May 1981

TABLE 1
Model characteristics

MODEL	TYPE	FUSELAGE				FUSELAGE + WING				
		L (m)	D (m)	ϵ^* (%)	B.L. o) PLATE (mm)	WING MATERIAL	b,b/2 (m)	\bar{c} (m)	ϵ^* (%)	S_{ref} (m ²)
1C	FULL	1.19	.13	.43	-	DURAL	1.27	.13	.84	.15
1H	HALF	2.70	.30	1.26	8	STEEL	1.44	.29	2.25	.38
2C	FULL	1.36	.13	.43	-	DURAL	1.27	.13	.84	.15
2H	HALF	2.07	.22	.67	22.5/6.5	STEEL	1.06	.21	1.31	.20
3C	FULL	1.21	.14	.54	-	STEEL	1.16	.15	1.0	.15
3H	HALF	2.86	.35	2.37	73/4	DURAL	1.38	.36	3.9	.43
4C	FULL	1.19	.14	.54	-	DURAL	1.14	.15	1.0	.14
4H	HALF	2.82	.35	2.37	73/4	DURAL	1.36	.35	3.9	.41
5C	FULL	1.40	.16	.61	-	DURAL	1.36	.15	1.19	.18
5H	HALF	2.70	.34	2.05	22.5/7.5	STEEL	1.45	.32	3.07	.42

*) in % of tunnel cross-section (3.2 m²) inclusive of b.l. plate (solid blockage)

o) second figure gives the gap width (mm)

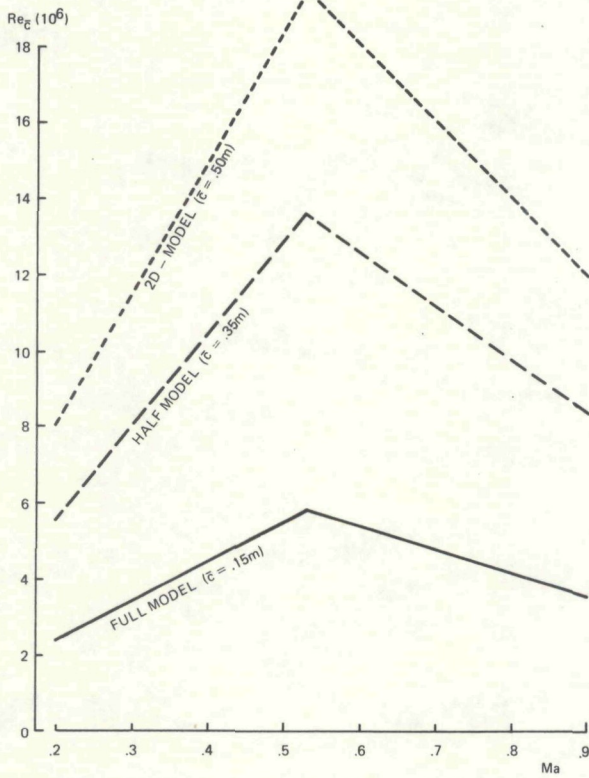


Fig. 1 Reynolds number capability

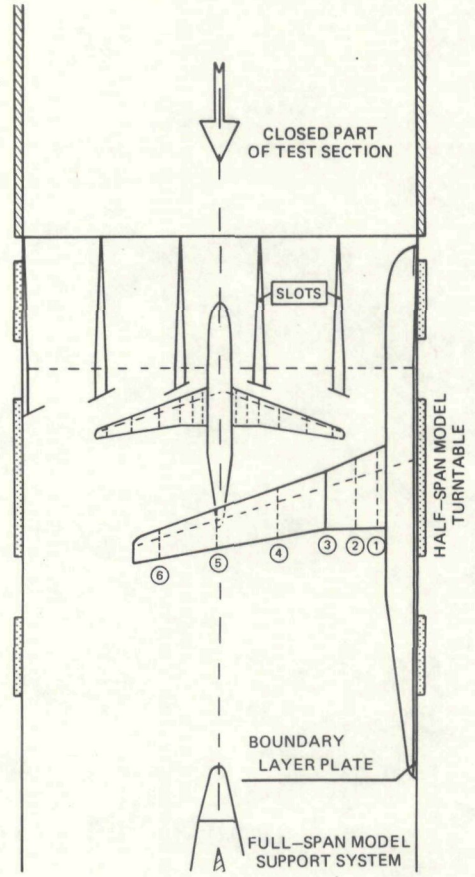


Fig. 2 Typical full- and half-models

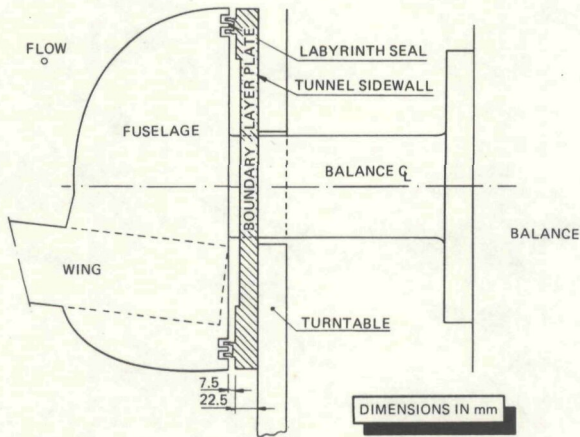


Fig. 3 Details of half-model mounting

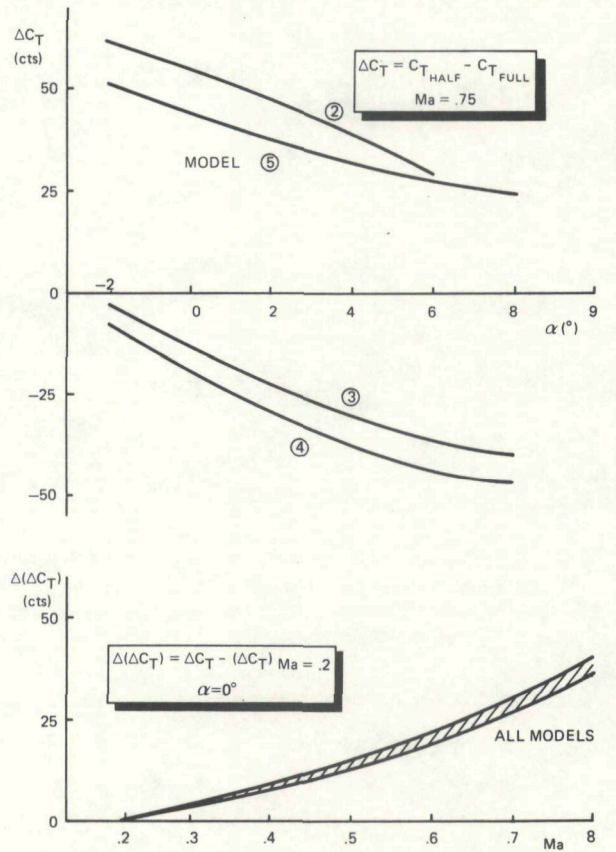


Fig. 4 C_T -differences of fuselage-only configurations

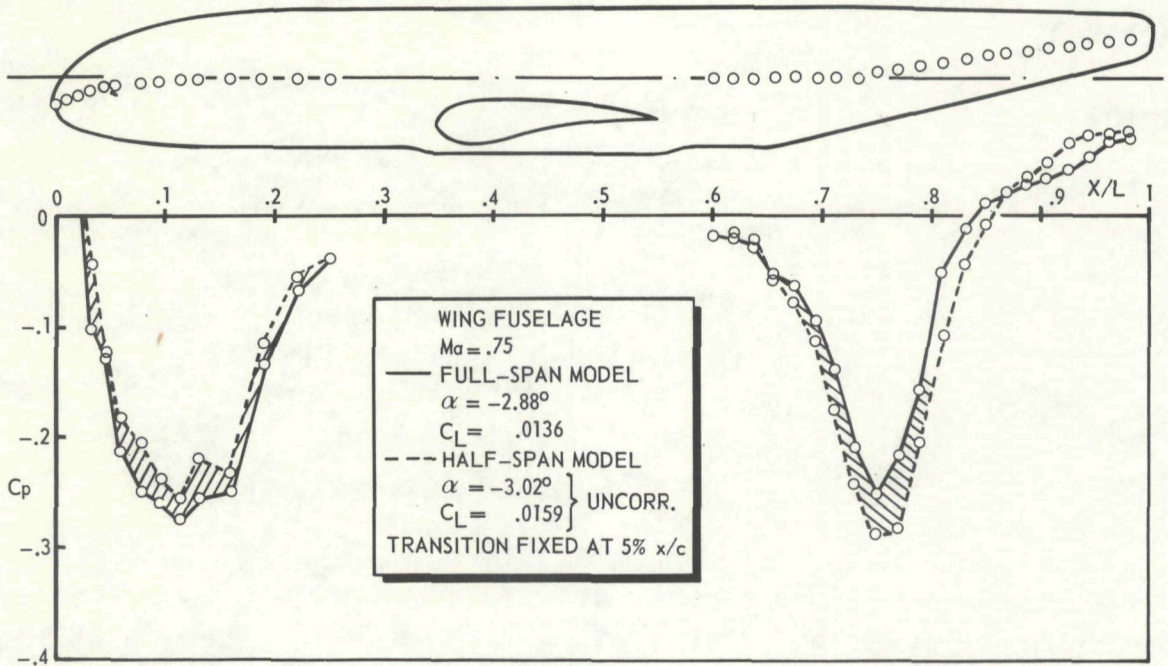


Fig. 5 Pressure distribution at zero-lift condition along fuselage

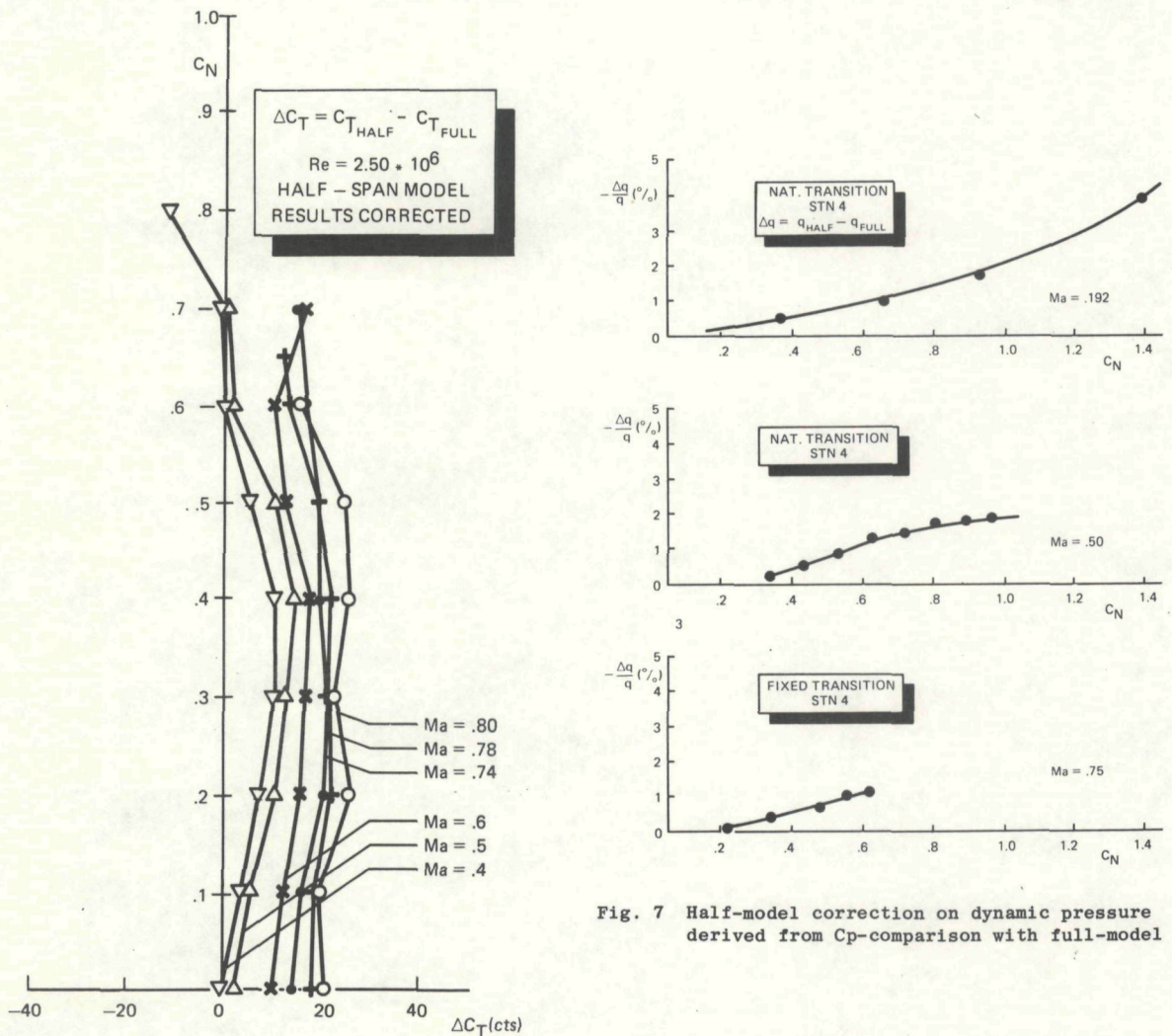


Fig. 7 Half-model correction on dynamic pressure derived from Cp-comparison with full-model

Fig. 6 Residual differences in tangential force coefficients of a typical wing-fuselage configuration

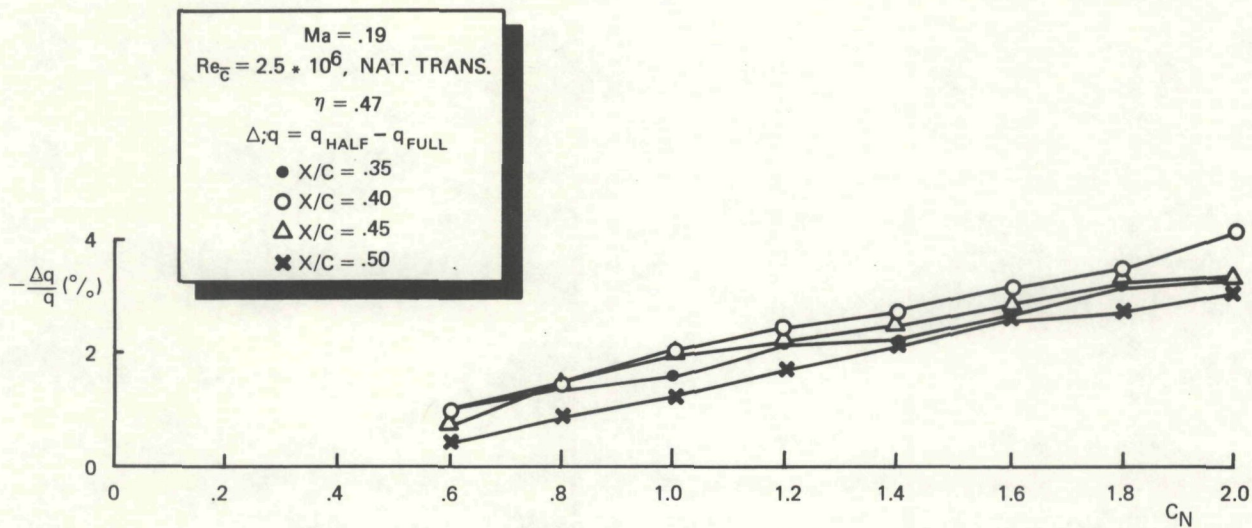


Fig. 8 Half-model q-correction derived from Cp-comparison with full model

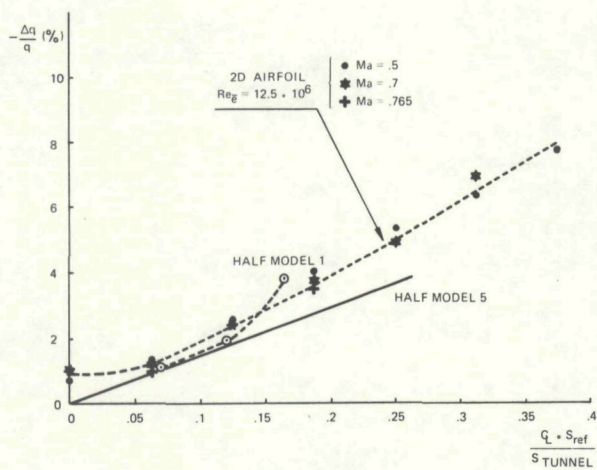


Fig. 9 Wall-interference effect on dynamic pressure

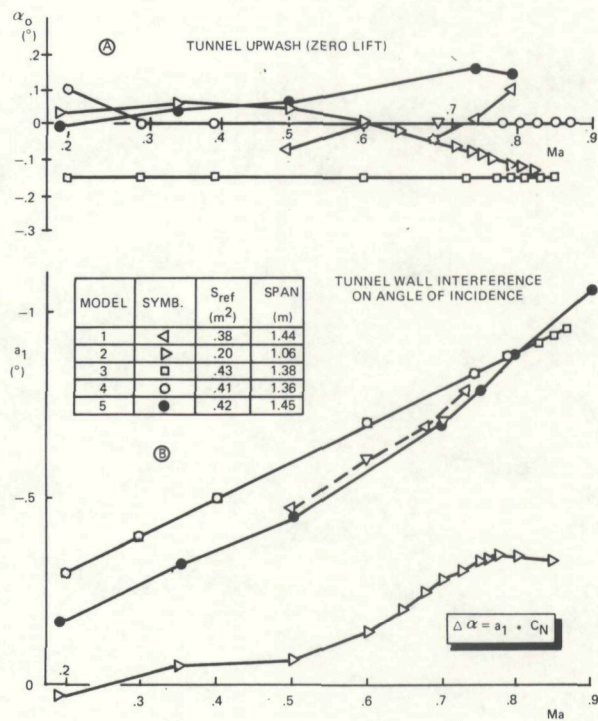


Fig. 10 Tunnel upwash and wall interference effect on incidence for various half-span models

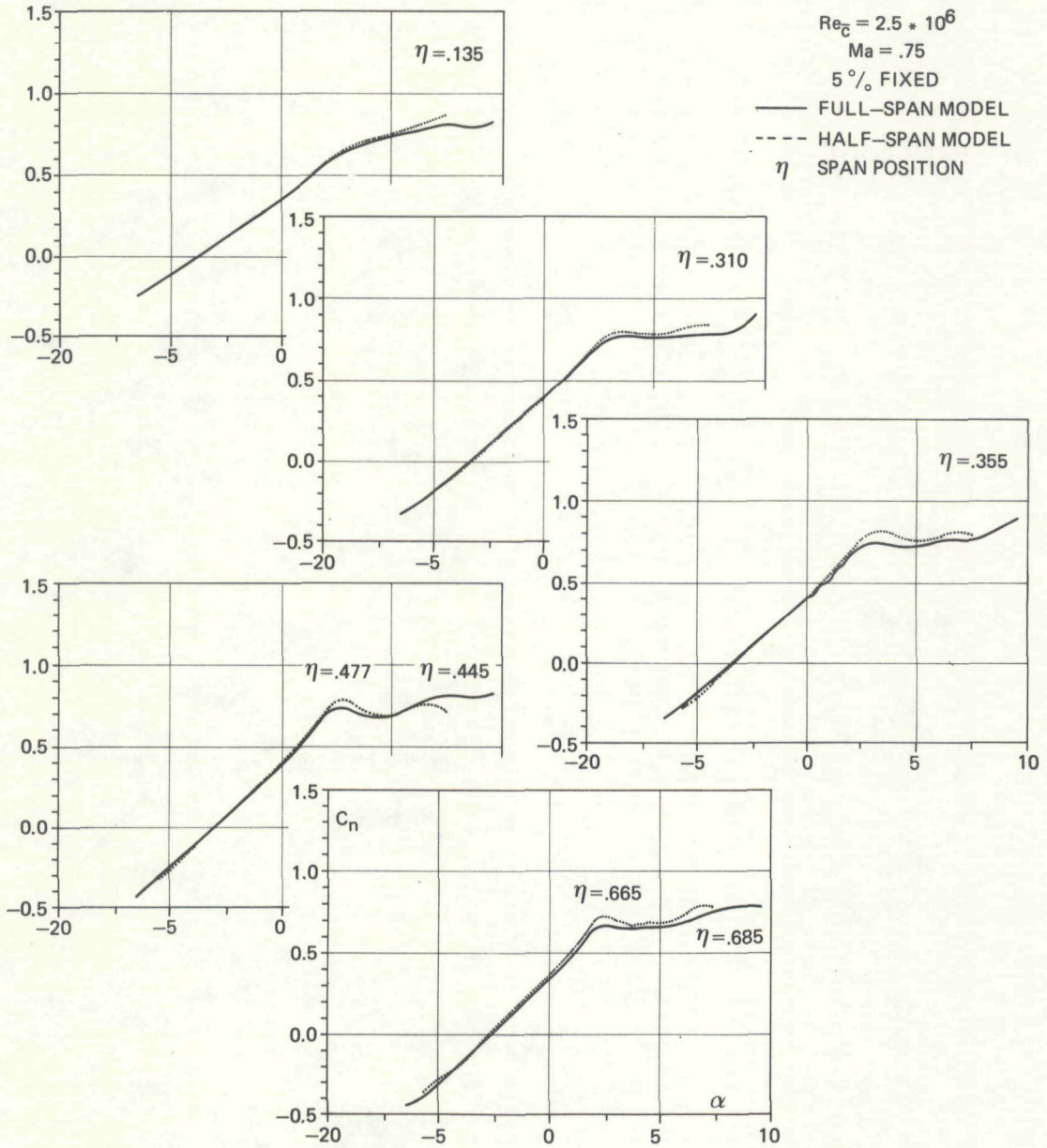


Fig. 11 Spanwise normal force distribution on half- and full-model

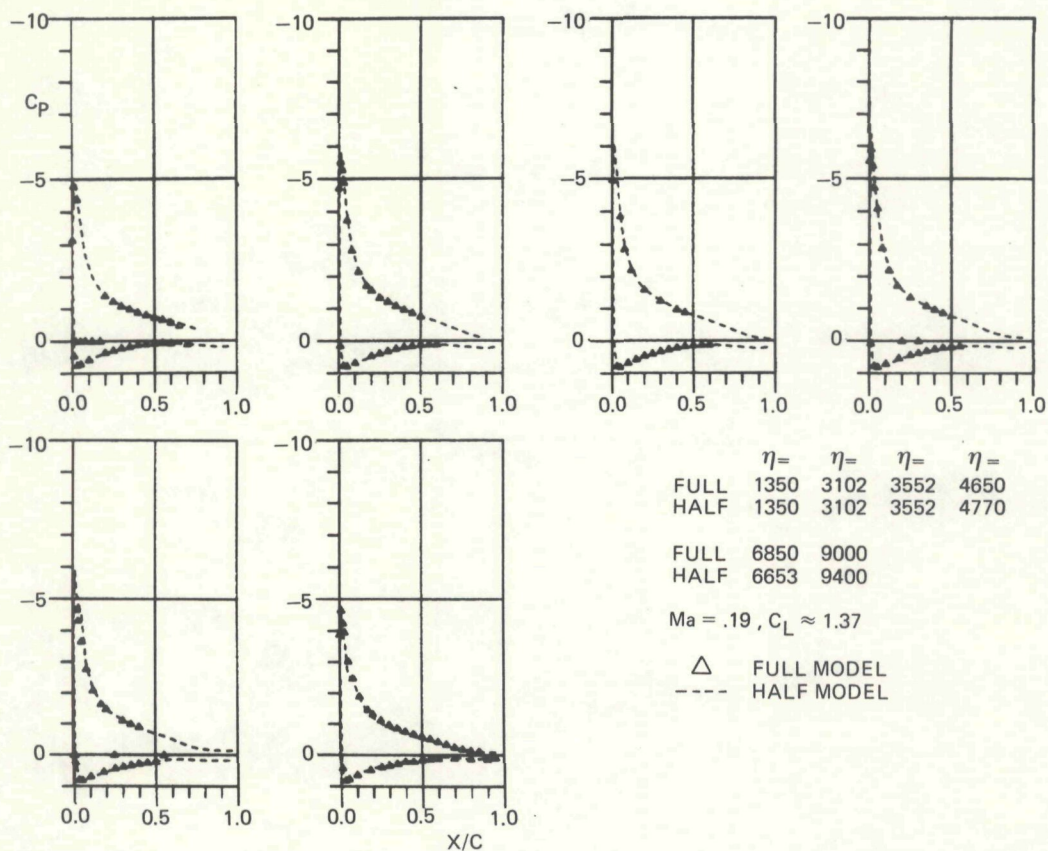


Fig. 12 Comparison of local pressure distributions

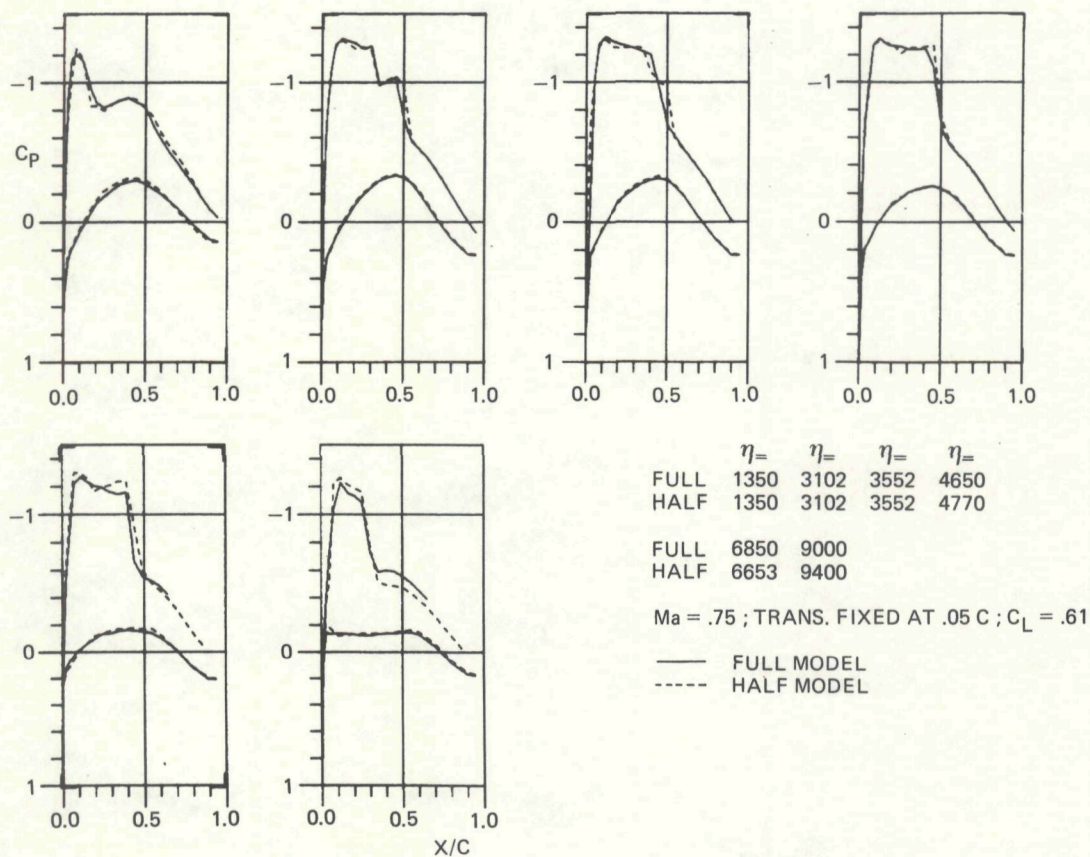


Fig. 13 Comparison of local pressure distributions

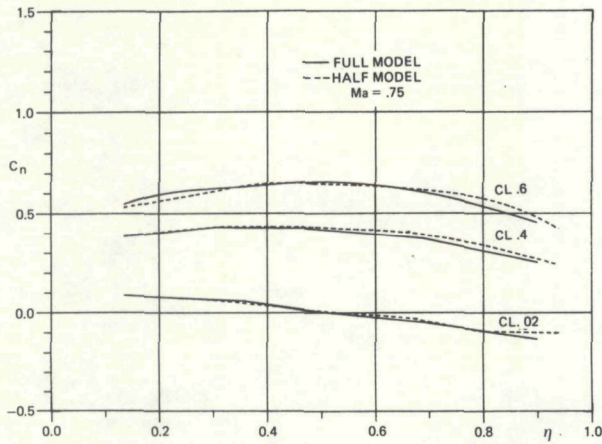


Fig. 14 Comparison of spanwise load distribution

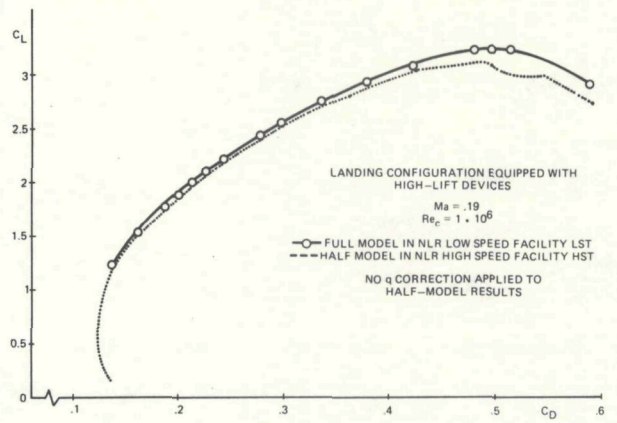


Fig. 15 Configuration equipped with high-lift devices

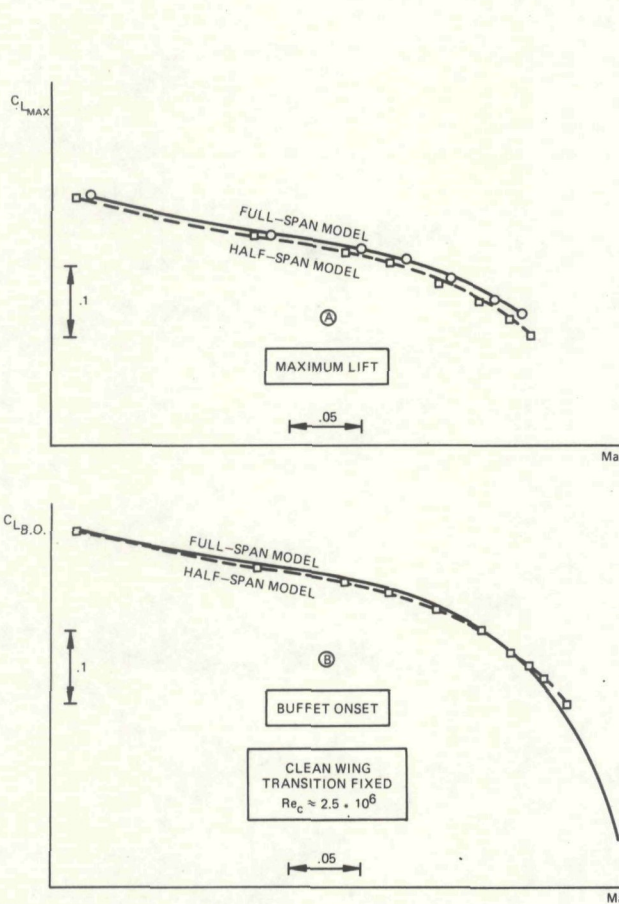


Fig. 16 Comparison of $C_{L_{max}}$ and buffet-onset boundaries

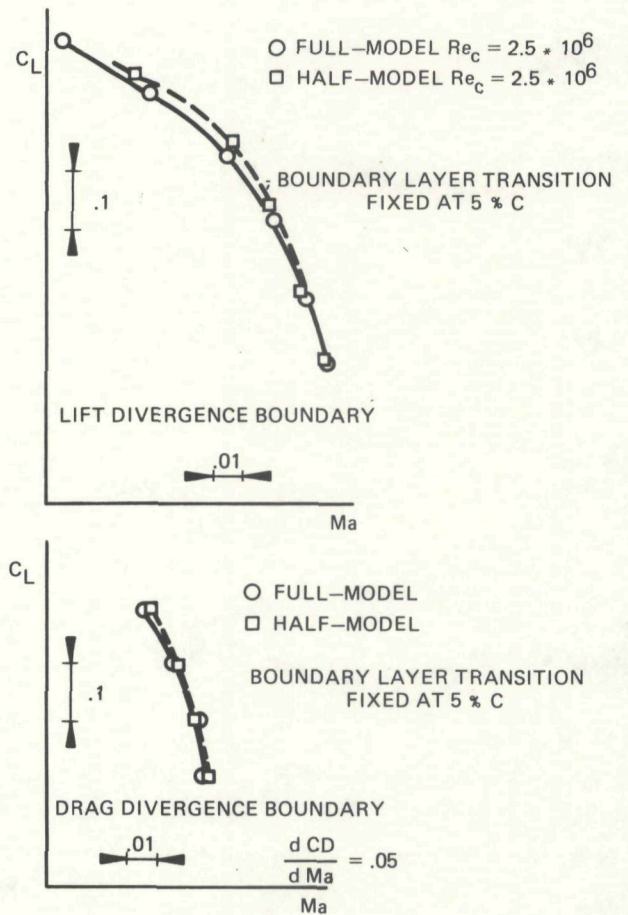


Fig. 17 Comparison of lift and drag divergence boundaries

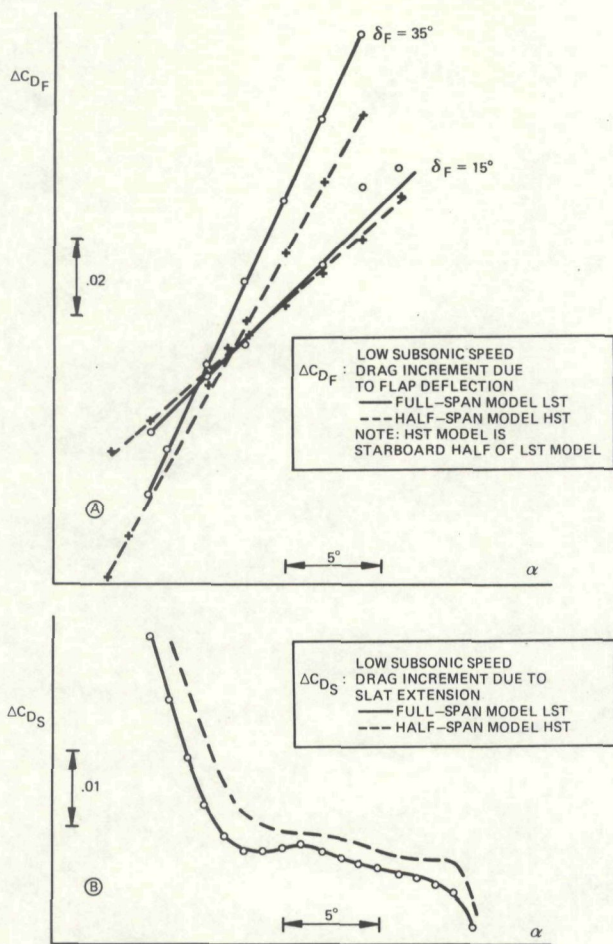


Fig. 18 Comparison of low-speed drag increments of full-span and half-span model with high-lift devices

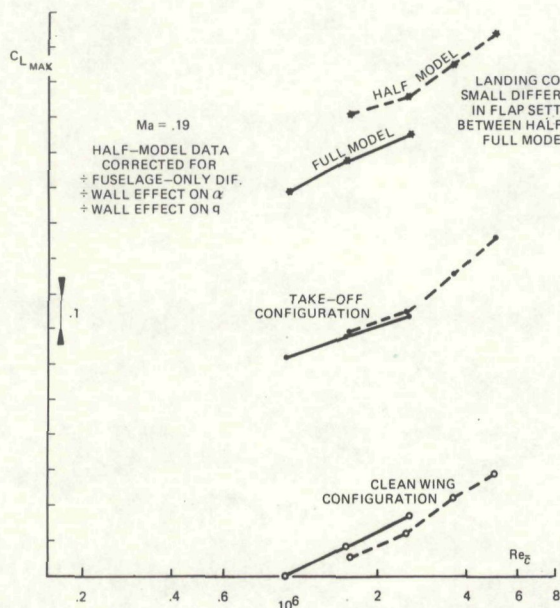


Fig. 20 Comparison of Reynolds number trends for low-speed maximum lift

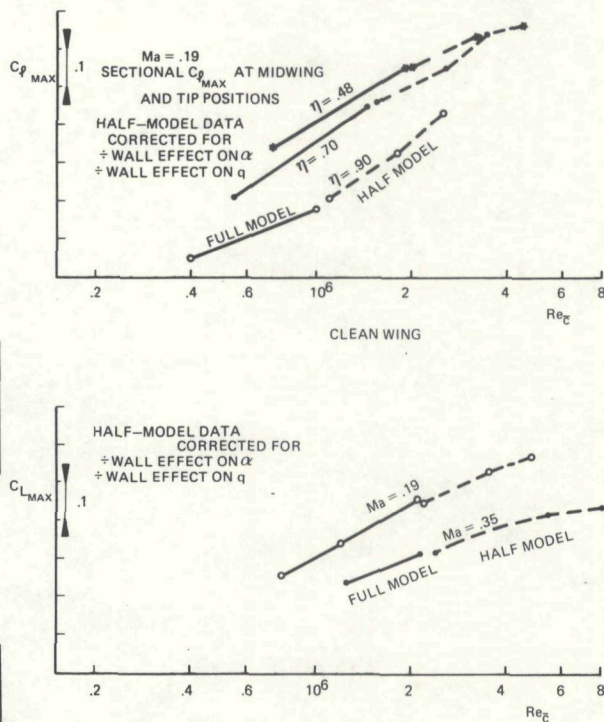


Fig. 19 Comparison of Reynolds number trends in local and overall maximum lift

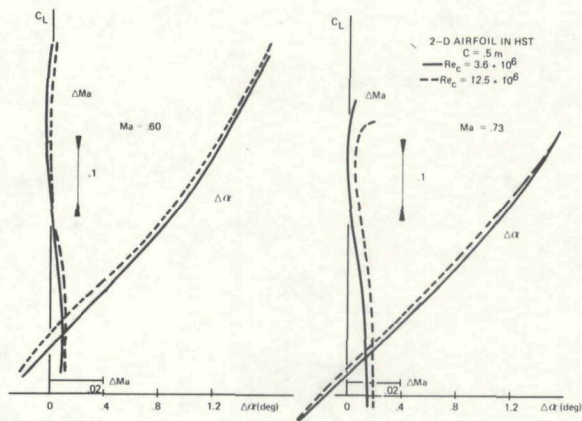


Fig. 21 Blockage correction (ΔMa) and incidence correction ($\Delta \alpha$) calculated from measured top and bottom wall pressure distributions

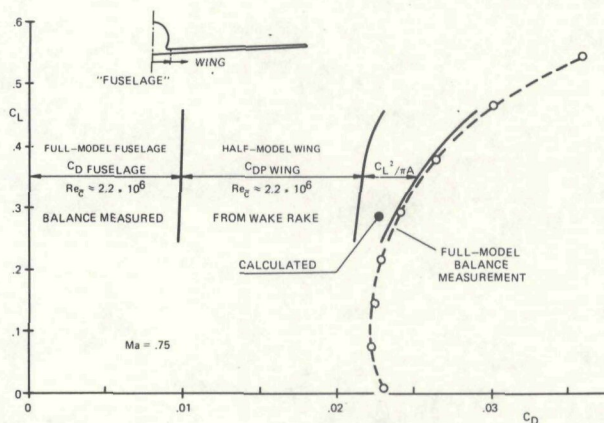


Fig. 22 Example of drag brake-down

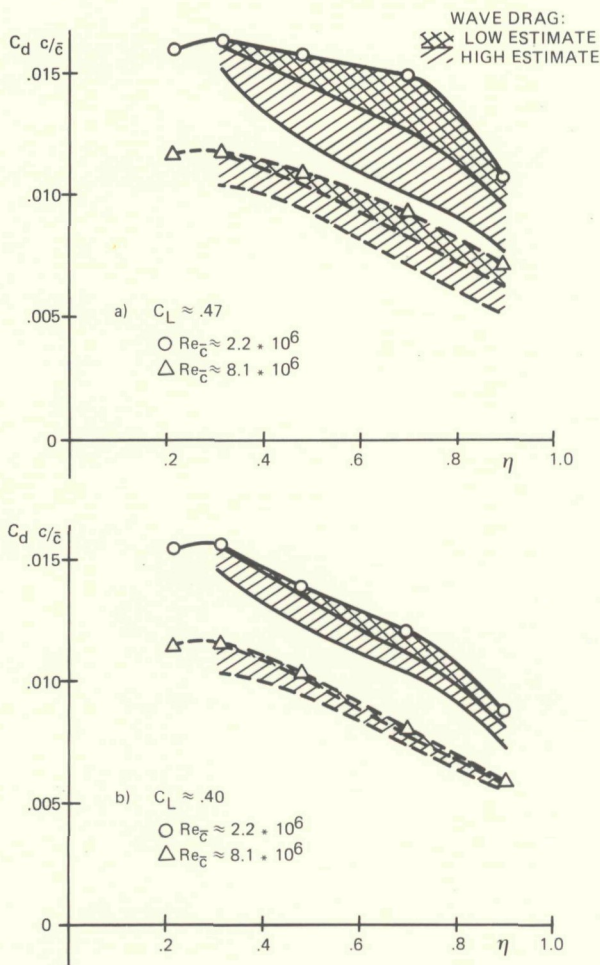


Fig. 23 Example of wake-drag analysis near design condition

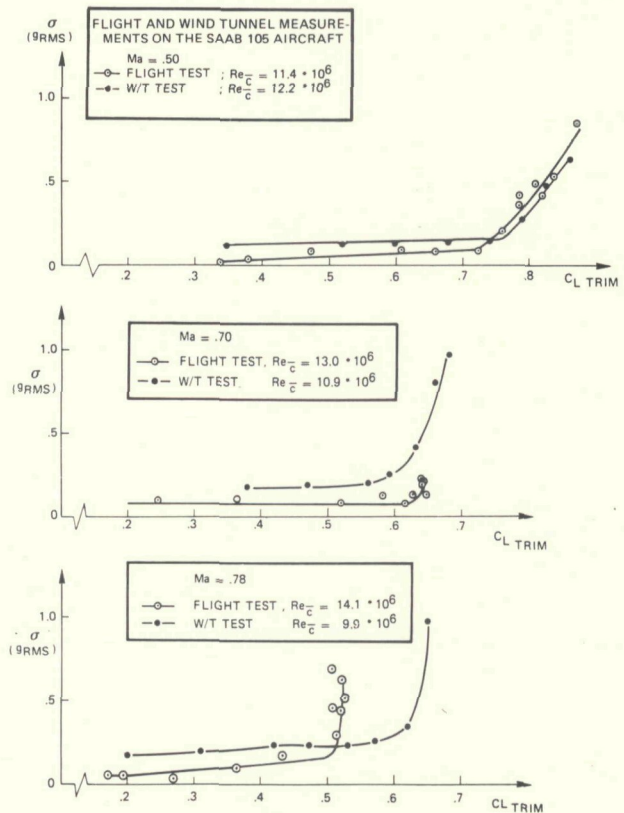


Fig. 24 Comparison of right wing tip accelerometer output from flight and wind tunnel test

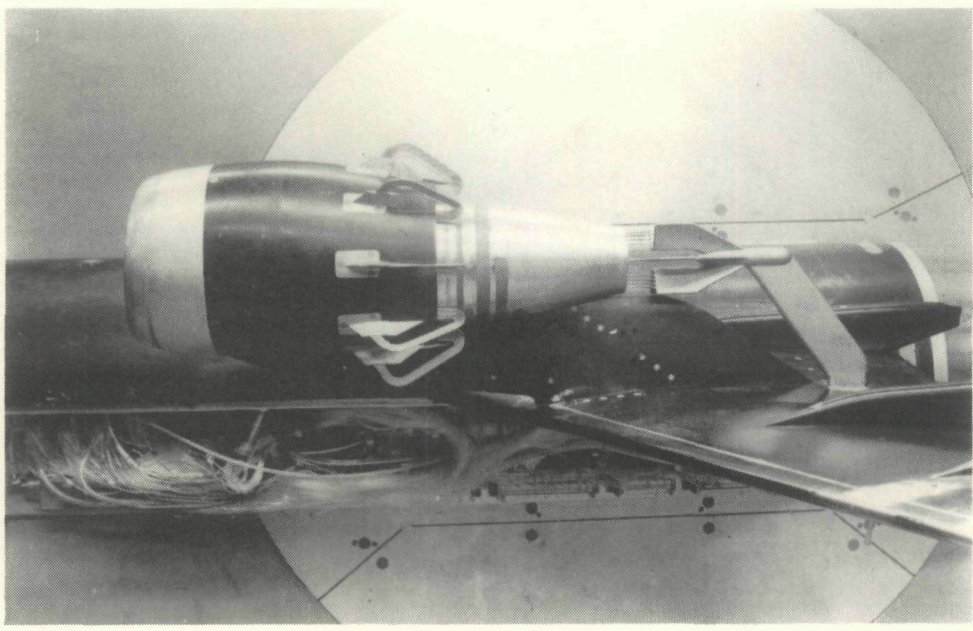


Fig. 25 Instrumented nacelle for mass flow testing

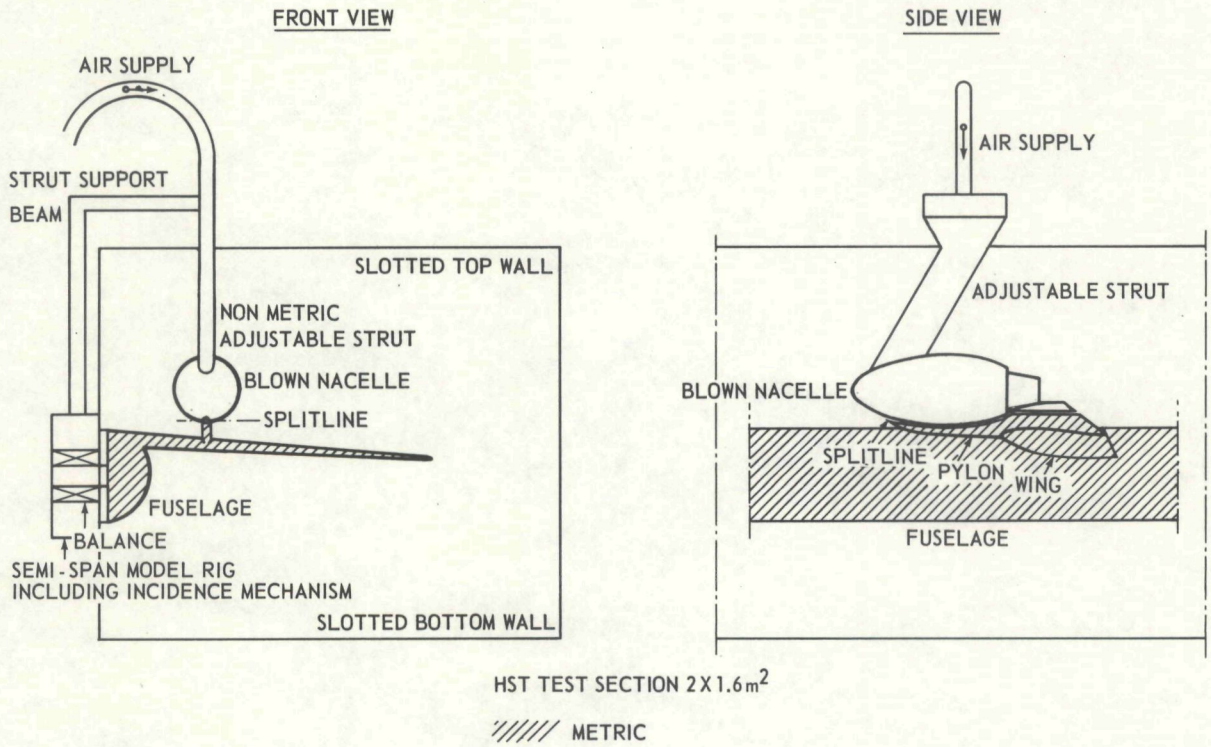


Fig. 26 Test setup with blown nacelle for optimisation of engine position

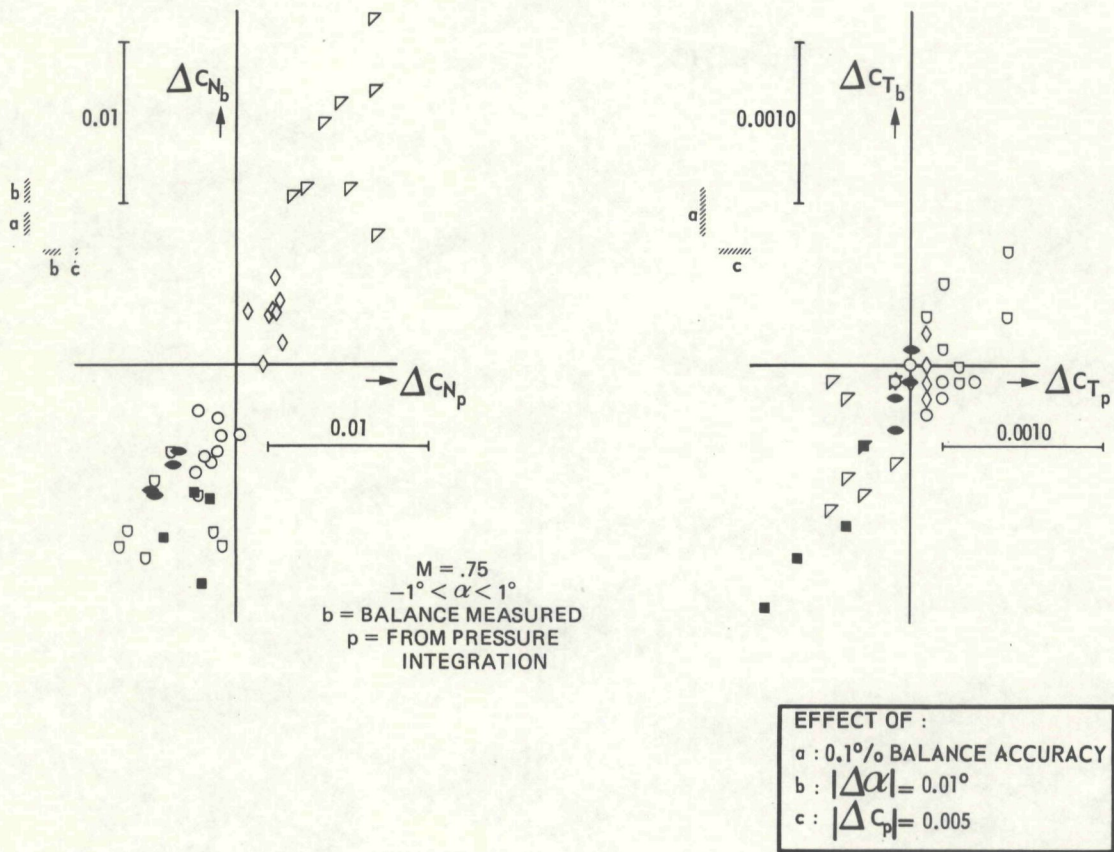


Fig. 27 Correlation of balance force and pressure force increments for test setup of figure 26